^{1}H-NMR Evidence for a Different Response to the Same Dose (2 Gy) of Ionizing Radiation of MG-63 Human Osteosarcoma Cells and Three-dimensional Spheroids

MARIA TERESA SANTINI[1,2], ROCCO ROMANO[2,3], GABRIELLA RAINALDI[1,2], ANTONELLA FERRANTE[1], PAOLA INDOVINA[1], ANDREA MOTTA[2,4] and PIETRO LUIGI INDOVINA[2,5]

[1]Dipartimento di Ematologia, Oncologia e Medicina Molecolare, Istituto Superiore di Sanità, Viale Regina Elena, 299, 00161, Rome;
[2]CNR-INFM, Unità di Napoli, Complesso Universitario Monte S. Angelo, Via Cinthia, 80126, Naples;
[3]Dipartimento di Scienze Farmaceutiche, Università degli Studi di Salerno, Via Ponte Don Melillo, 84084, Fisciano, Salerno;
[4]Consiglio Nazionale delle Ricerche, Istituto di Chimica Biomolecolare, Comprensorio A. Olivetti, Edificio 70, Via Campi Flegrei, 34, 80078 Pozzuoli, Naples;
[5]Dipartimento di Scienze Fisiche, Università di Napoli "Federico II", Complesso Universitario Monte S. Angelo, Via Cinthia, 80126, Naples, Italy

Abstract. *High resolution proton nuclear magnetic resonance (^{1}H-NMR) spectroscopy was used to examine the response of the MG-63 osteosarcoma cell line grown in monolayer and as 3-dimensional tumor spheroids to the same low dose (2 Gy) of ionizing radiation. The MG-63 cells and spheroids were irradiated at 24 h of growth and the ^{1}H-NMR spectra of whole control and irradiated monolayer cells and of whole control and irradiated multicellular spheroids collected after another 24 h were compared. The ^{1}H-NMR spectra of the perchloric acid extracts as well as the 2-dimensional ^{1}H-NMR spectra of both pairs of cell systems were also obtained. Possible radiation-induced cell damage was determined by lactate dehydrogenase (LDH) release and variations in cell growth, while cell death was evaluated by chromatin dye Hoechst staining and DNA fragmentation assays. The results demonstrated that no cell damage took place, but that significant variations in numerous metabolites occured in both the monolayer cells and the spheroids after irradiation. Most of the changes observed were very similar in nature. In fact, significant increases in lactate, alanine, creatine and phosphocreatine and choline-containing metabolites and a significant decrease in glutathione (GSH) were observed in both cells and spheroids. However, while significant increases in CH_2 and CH_3 mobile lipids, glutamine/glutamate, taurine and inositol were seen in the spheroids, no variations in CH_2 or CH_3 lipids, glutamine/glutamate or taurine were recorded in the MG-63 cells grown in monolayer after irradiation. In addition, a significant decrease rather than a significant increase in inositol was also noted in the monolayer cells. The data presented seem to suggest that, although neither monolayer cells nor spheroids show apparent signs of damage after exposure to the same dose of ionizing radiation, very different cell death responses as well as very diverse antioxidant/osmoregulatory reactions were triggered by this stressing agent.*

In vitro cancer studies have been conducted principally by using stabilized tumor cell lines grown in monolayer. Although this *in vitro* cell model has yielded valuable information regarding the mechanisms of malignant growth, it is, nonetheless, unsuitable for representing completely *in vivo* tumors. Solid tumors grow in a 3-dimensional spatial array and cells in these tumors are exposed to non-uniform distributions of oxygen and nutrients as well as to other physical and chemical stresses. Consequently, because of the great microenvironmental variations present in different regions of tumors, significant cellular heterogeneity may result. Therefore, it is obvious that cells grown in monolayer, which are exposed to the same oxygen and nutrient concentrations, cannot be utilized to investigate all aspects of tumor biology. Thus, in order to design more

Correspondence to: Maria Teresa Santini, Dipartimento di Ematologia, Oncologia e Medicina Molecolare, Istituto Superiore di Sanità, Viale Regina Elena, 299, 00161, Rome, Italy. Tel: +39-06-4990-3194, Fax: +39-06-4938-7140, e-mail: santini@iss.it

Key Words: Three-dimensional tumor spheroid, high resolution nuclear magnetic resonance spectroscopy, apoptosis, osmoregulation, ionizing radiation.

suitable *in vitro* systems that take into consideration the 3-dimensional arrangement of solid tumors, multicellular tumor spheroids were developed. Tumor spheroids represent quite realistically the 3-dimensional growth and organization of solid tumors and, consequently, simulate much more precisely the cell-cell interactions and microenvironmental conditions found in these tumors (1, 2).

High resolution proton nuclear magnetic resonance (^{1}H-NMR) spectroscopy can be used to non-invasively examine various aspects of tumor biology in cells grown in monolayer and in 3-dimensional tumor spheroids. This technique has been utilized to study tumor cell growth (3), the efficacy of anticancer drugs (4) and cholesterol metabolism (5) in monolayer cultures, as well as drug toxicity (6) in 3-dimensional tumor spheroids. As is apparent from these and other studies, important information regarding cell function and cellular response to different stressing agents can be obtained by this technique.

It has been demonstrated that ionizing radiation can induce numerous effects in cells including changes in metabolism (7), cell cycle delay (8), damage to DNA (9) and the cell membrane (10) and, ultimately, necrosis and apoptosis (11). In addition, it has also been shown that the type of cell growth, *i.e.*, in monolayer or as 3-dimensional tumor spheroids, can also play a pivotal role in the cellular response to ionizing radiation. It has been observed that cells grown in monolayer or as 3-dimensional tumor spheroids respond in a completely different manner to ionizing radiation (12, 13). In particular, the apoptotic response can vary dramatically depending upon the type of cell culture system utilized (14). In this study, much less apoptosis was seen in NIH:OVCAR 3 spheroids than in the same cell line grown in monolayer. These investigators, as well as many others, have hypothesized that cell contact (15, 16) and/or extracellular matrix (ECM) communication (2, 17), both of which are much more active in spheroids, are determinant in the differences in resistance observed.

It was the purpose of the present report to examine the response of the MG-63 osteosarcoma cell line grown in monolayer and as 3-dimensional tumor spheroids to the same low dose (2 Gy) of ionizing radiation using ^{1}H-NMR spectroscopy. Consequently, the MG-63 cells and spheroids were irradiated at 24 h of growth and the ^{1}H-NMR spectra of whole control and irradiated monolayer cells and of whole control and irradiated multicellular spheroids were collected after another 24 h. The spectra were then compared using an algorithm developed by our group (18). The ^{1}H-NMR spectra of the perchloric acid extracts as well as the 2-dimensional ^{1}H-NMR spectra of both pairs of cell systems were also obtained. Possible radiation-induced cell damage was determined by lactate dehydrogenase (LDH) release and variations in cell growth (*i.e.*, determination of total protein content), while cell death was ascertained by chromatin dye Hoechst staining and DNA fragmentation assays. However, since cell proliferation is not only an important indicator of cell damage, but differences in cell growth can also alter ^{1}H-NMR results (3, 19, 20), it was necessary to monitor this parameter very precisely. Consequently, various methods were attempted. The disaggregation of spheroids into single cells that are then counted, a procedure often used in these types of studies, was conducted but resulted in a high percentage of cell loss and, thus, had to be excluded. Only total protein determinations gave reproducible data. The results demonstrated that no cell damage took place, but that significant variations in numerous metabolites occurred in both monolayer cells and spheroids after irradiation. Most of the changes observed were very similar in nature. In fact, significant increases in lactate, alanine, creatine and phosphocreatine and choline-containing metabolites and a significant decrease in glutathione (GSH) were observed in both cells and spheroids. However, while significant increases in CH_2 and CH_3 mobile lipids, glutamine/glutamate, taurine and inositol were seen in spheroids, no variations in CH_2 and CH_3 lipids, glutamine/glutamate and taurine were recorded in MG-63 cells grown in monolayer after irradiation. In addition, a significant decrease rather than a significant increase in inositol was also noted in monolayer cells. The relevance of these results, especially with respect to possible differences in cell death processes and antioxidant/osmoregulatory responses of the two cell models, will be discussed.

Materials and Methods

Monolayer cells. The MG-63 cells (a human osteosarcoma cell line) purchased from the Istituto Zooprofilattico Sperimentale della Lombardia e dell'Emilia (Brescia, Italy) were grown in monolayer in tissue culture flasks (Nunc A/S, Roskilde, Denmark) containing RPMI 1640 (Gibco BRL, Burlington, ON, Canada) supplemented with 10% heat-inactivated fetal bovine serum (FBS Characterized; Hyclone, Utah, USA), non-essential amino acids, 100 I.U./ml penicillin and 100 μg/ml streptomycin (Gibco BRL) and incubated at 37˚C in a 5% CO_2 atmosphere. Aliquots of the same batch of frozen cells were thawed and used for all experiments at about the same number of passages (between 10 and 15 passages) so as to make certain that no major variations in the cell populations had occurred between each trial. All products not specified were purchased from Sigma Chemical Co. (St. Louis, MO, USA).

Multicellular tumor spheroids. In order to form spheroids by using the liquid-overlay technique, the MG-63 cells, grown in monolayer as described above, were detached from the substratum by first adding 10 mM EDTA (pH 7.4) and, once this solution had been removed, by adding 0.25% trypsin. The cells were then seeded in 6-well tissue culture plates (Nunc A/S) to which a 3% agar dissolved in complete medium (RPMI plus 10% FBS) had previously been added to the bottom of the wells and had solidified. To each well were added $1.25x10^5$ cells/ml ($5.0x10^5$ cells/well) and the plates were incubated at 37˚C in a 5% CO_2 atmosphere.

Irradiation protocol. After 24 h of growth, both monolayer cells and spheroids were irradiated with a dose of 2 Gy directly in the tissue culture plates at room temperature using a Cobalt-60 irradiation unit (Gammacell 220, Atomic Energy of Canada Ltd.) at a dose rate of approximately 3.9 Gy/min. The irradiation was conducted at 24 h of growth since at this time the spheroids were already well-formed. The control monolayer and spheroid cultures were kept at room temperature under the same conditions as the experimental ones. Both the monolayer cells and spheroids were collected after irradiation at the times specified for the experiments described below.

Evaluation of cell damage

Lactate dehydrogenase (LDH) release: In order to determine whether the MG-63 monolayer cells and spheroids were damaged, the intracellular and extracellular quantity of LDH in controls and in these cells and spheroids exposed to 2 Gy of ionizing radiation was determined using a Cytoxicity Detection Kit (LDH) (Roche Diagnostics, Penzberg, Germany). In particular, for monolayer cells, the growth medium was removed and the cells were detached by scraping, collected and placed on ice. The spheroids and their medium were collected directly and placed on ice. Both monolayer cells and spheroids were then centrifuged at 380 xg for 5 min. The supernatants were used to determine the quantity of LDH released and found outside the cells and spheroids, while the pellets were resuspended in 1 ml PBS (pH 7.4) and sonicated on ice. After sonication, the samples were centrifuged and the supernatants collected in order to establish the quantity of intracellular LDH. Enzyme activities were determined spectrophotometrically using a Novapath microplate reader (BIO-RAD Laboratories, Inc., Milan, Italy) at 6 and 24 h after the end of exposure by measuring the change in optical density at 490 nm. These 2 time-points were chosen since it is not known whether eventual cell damage can occur at short or longer times after exposure. At least 9 samples from 3 independent experiments were examined.

Growth assessment by total protein determination: In order to evaluate cell growth in the MG-63 monolayer cells and spheroids, the total protein content was determined. Briefly, after 0, 24, 48 and 72 h of growth, the monolayer cells and spheroids were washed twice in PBS (pH 7.4) and lysed by incubation at 50˚C in Laemli buffer (60 mM Tris-HCl, pH 6.8; 2% SDS) for 5 min and stored at –20˚C until use. Protein determination was conducted using the Bio-Rad DC protein assay (BIO-RAD Laboratories, Inc.) following the manufacturer's instructions. The protein content was determined spectrophotometrically using a Novapath microplate reader (BIO-RAD Laboratories, Inc.) by measuring the change in optical density at 750 nm. Bovine serum albumin (BSA) was used as standard. At least 10 samples from 3 independent experiments were examined.

Preparation of perchloric acid extracts of MG-63 monolayer cells and spheroids. In order to prepare the extracts, approximately $35x10^6$ MG-63 monolayer cells and MG-63 spheroids also containing about $35x10^6$ cells were collected 24 h after irradiation from the tissue culture flasks. The monolayer cells were detached using 10 mM EDTA (pH 7.4) and 0.25% trypsin, centrifuged, washed twice with cold PBS (pH 7.4) and the supernatants removed. The spheroids were collected, washed twice with PBS (pH 7.4) and the supernatants also removed. To both the cell and spheroid pellets was added a 30% perchloric acid solution (equal to twice the pellet volume) and the resulting cell suspensions were kept at room temperature for 30 min. The perchloric acid was neutralized by adding K_2CO_3 until a pH of about 7.4 was reached. The solution was centrifuged at 200 xg for 5 min and the supernatant was centrifuged again at 16,000 xg for 2 min. This second supernatant was removed and stored at –80˚C for about 2 h and was then lyophilized overnight at –50˚C. The samples were stored at 4˚C until NMR measurement.

One-dimensional ^{1}H-NMR measurements of whole MG-63 monolayer cells and spheroids and the perchloric acid extracts of both cells and spheroids at 500 MHz. For the ^{1}H-NMR measurements, the MG-63 cells and spheroids containing about $35x10^6$ cells were used. The monolayer cells were collected from the tissue culture plates by detachment using 10 mM EDTA (pH 7.4) and 0.25% trypsin, were centrifuged, washed 3 times with PBS (pH 7.4) and resuspended in 1.0 ml of the same buffer. The spheroids were collected from the plates 24 h after irradiaton, washed 3 times with PBS and resuspended in 1.0 ml of the same buffer. To both monolayer cells and spheroids were also added 4 µl of a 21.8 mM TSP (sodium 3-trimethylsilyl(2,2,3,3-D_4) propionate) solution used as internal standard and 10 µl of D_2O. The high resolution ^{1}H-NMR spectra were recorded under fully relaxed (T1) conditions on a Bruker DRX-500 spectrometer operating at 500 MHz using an inverse multinuclear probehead fitted with gradients along the X-, Y- and Z-axes. The measurements were performed in spinning NMR tubes at a probe temperature of 300 K in the presence of about 15% of D_2O used as a lock signal. Manual and automatic shimming were performed immediately before each measurement. The ^{1}H free induction decays (FIDs) of cells and spheroids were obtained with a 9 µs pulse delay (90˚ flip angle), a ±4006.4 Hz (±8 ppm) spectral window and 8 K data-points. The relaxation delay between scans was set at 5.0 s and the acquisition time was 1.2 s. Therefore, the recycling time was 6.2 s. The intensity of the water signal was reduced by incorporating the excitation sculpting sequence for water suppression. A pulsed-field gradient double echo with a soft square pulse of 4 ms at the water resonance frequency, with the gradient pulses of 1 ms each in duration, were used (21). Each spectrum represented the sum of 128 FIDs. The measured FIDs were zero-filled to 64 K and Fourier transformed without apodization to the frequency domain. The spectra were manually phase-corrected (zero and first order) and finally a spline baseline correlation was applied. Resonance chemical shifts were expressed in ppm in reference to the internal standard TSP assigned to 0 ppm (22, 23). The spectral lines were analyzed by fitting them with Lorentzian shape lines (the MacFID 5.5 program was used). At least 5 independent experiments were conducted for both MG-63 monolayer cells and spheroids.

The preparation of each sample and the subsequent NMR measurement lasted about 20 min. However, despite this short measurement time and since a perfusion system was not used, it was necessary to determine the stability of the NMR spectra of the cells and spheroids over time; the spectra remained very stable for about one hour.

For the perchloric acid extract measurements, the stored lyophilized powder was resuspended in D_2O and the pH was adjusted to about 7.4 with DCl or NaOD and 4 µl of a 21.8 mM TSP solution was added. The high resolution proton NMR spectra were obtained at 300 K in the same manner as that of whole cells and spheroids except that, for the extracts, pre-saturation of the water signal was used rather than the sculpting water suppression sequence. Again, 5 independent experiments were conducted for both cells and spheroids.

Normalization algorithm. In order to obtain relative quantitative information between control and exposed MG-63 monolayer cells and of control and irradiated MG-63 spheroids, a comparison of intensities was conducted by normalization of the spectra using the MiRaNAl algorithm (20). The algorithm is based on the assumption that differences in signal intensities result in proportional variations of spectral intensities due to differences in cell number, while non-proportional changes may most likely be attributed to true differences in sample metabolites. The proportional variations are described by a normalization factor R, which must be calculated in order to compare the signal intensities of two samples. The MiRaNAl algorithm consists of minimizing the rank of a Hankel matrix constructed with the differences of the free induction decay signals, one of which is multiplied by R_{test}, where R_{test} is the test value for R estimation. When the FIDs are correctly normalized, that is when $R_{test}=R$, the differences do not contain the proportional signal intensities, but rather only the non-proportional part of the signal intensities. The rank of the Hankel matrix is approximately equal to the number of signals, such that when $R_{test}=R$, the rank of the Hankel matrix is at a minimum.

Normalization of spectra obtained from extracts was not conducted by the MiRaNAl algorithm, but rather with the TSP internal standard (24).

Two-dimensional ^{1}H-NMR measurements of whole MG-63 monolayer cells and spheroids at 500 MHz. Homonuclear clean 2-dimensional total correlation spectroscopy (TOCSY) (25, 26) spectra of MG-63 monolayer cells and spheroids at 24 h after irradiation were recorded by using the time-proportional phase incrementation of the first pulse (27), and incorporating the excitation sculpting sequence (21) for water suppression. A pulsed-field double echo with a soft square pulse of 4 ms at the water resonance frequency, with the gradient pulse of 1 ms each in duration, was applied. For each experiment, 512 equally spaced evolution time-period T1 values were acquired, averaging 16-64 transients of 2048 points, with 6024 Hz of spectral width. Time-domain data matrices were zero-filled to 4 K in both dimensions, thus yielding a digital resolution of 2.94 Hz/pt. Prior to Fourier transformation, a Lorentz-Gauss window with different parameters was applied for both T1 and T2 dimensions for all experiments. TOCSY experiments were recorded with a spin-lock period of 0.064 and 0.096 s, achieved with the MLEV-17 pulse sequence (28). Furthermore, in order to compare 2-dimensional experiments, a mono-dimensional experiment with the same TOCSY acquisition parameters (*i.e.*, a relaxation delay between scans of 1.5 s, a transient point number of 2048 with 6024 Hz spectral width, a 90˚ pulse of 8.75 μs) followed by a TOCSY experiment were performed on the same sample. In this manner, the spectra could be normalized using the normalization algorithm described above for the 1-dimensional ^{1}H-NMR studies. The cross-peaks were integrated by using the specific routine of the XWINNMR Bruker software and, after normalization, the percent variations ((Irradiated – Control)/Irradiated x 100) were obtained.

Determination of apoptosis

Hoechst 33258 staining: Apoptosis was evaluated in the control and irradiated MG-63 monolayer cells and spheroids at 24 h after irradiation by fluorescent microscopy utilizing the chromatin stain Hoechst 33258 (Sigma). For monolayer cells, the growth medium was removed and the cells fixed with 3% formaldehyde for 10 min at room temperature. The cells were washed twice with PBS (pH 7.4), permealized with 0.5% Triton X-100 for 5 min also at room temperature and stained with 1 μg/ml of the chromatin dye Hoechst 33258 for 30 min at 37˚C. Spheroids were collected from the wells, centrifuged and fixed with 6% formalin in PBS (pH 7.4). After washing, the samples were dehydrated through graded ethanols up to 100%, placed in a 1:1 xylol/absolute ethanol mixture and then in absolute xylol. Finally, the spheroids were embedded in liquefied paraffin and left at room temperature until the paraffin hardened. Paraffin sections for light microscopy were obtained with an ultramicrotome (LKB, Nova) and stained utilizing the chromatin stain Hoechst 33258. Briefly, the sections were deparaffinized and hydrated through xylol and a graded alcohol series up to 30% ethanol. Sections were then placed in distillated water, incubated with 1 μg/ml Hoechst 33258 and mounted on glass coverslips with Permount. Both monolayer and spheroid samples were then observed and photographed with a Zeiss Axiovert fluorescence microscope. The percentage of apoptotic cells in monolayers was determined by counting at least 1000 cells in 10 randomly-chosen fields, while in spheroids the percentage of apoptotic cells was evaluated by counting at least 10 spheroids (for a total of at least 1500 cells) of each sample in randomly-selected areas.

Analysis of DNA fragmentation by gel electrophoresis: In order to separate high molecular weight chromatin from the nucleosomal DNA fragments after 48 h and 7 days, the monolayer cells were detached using 10 mM EDTA (pH 7.4) and 0.25% trypsin, washed twice with sterile PBS (pH 7.4) and lysed in 0.5 ml of lysis buffer (10 mM Tris, pH 7.4; 1 mM EDTA, pH 8.0; 0.2% Triton X-100) containing Proteinase K (100 μg/ml) for 2 h at 37˚C. The spheroids were collected, washed twice with PBS and also lysed in the same buffer under the same conditions. All samples were then centrifuged at 16,000 xg for 30 min. The DNA in the supernatant was precipitated with 5 N NaCl in 1 vol of isopropilic alcohol overnight at –20˚C. The DNA precipitates were recovered by centrifugation at 16,000 xg for 30 min, were air-dried for 20 min at room temperature, resuspended in TE buffer (10 mM Tris, pH 7.4; 1 mM EDTA, pH 8.0) containing RNAse (200 μg/ml) and incubated for 20 min at 65˚C. Before electrophoresis, loading buffer (Gel Loading Solution, Type I 6X, Sigma) was added to each sample. DNA was separated overnight by electrophoresis on

Table I. *Enzyme leaked values expressed as a percentage of total LDH enzyme (i.e., [extracellular]/{[extracellular]+[intracellular]}x100) of control monolayer MG-63 cells and spheroids and of these systems irradiated with 2 Gy, taken at 6 and 24 h after the end of exposure. As can be seen, no significant variations were observed in these values at either times tested ($p<0.05$). The means and standard deviations of at least 9 samples from 3 independent experiments are shown.*

	Control	2 Gy
Monolayer		
6 h	19.7±1.8	20.9±1.7
24 h	16.9±1.9	16.8±2.0
Spheroids		
6 h	19.8±7.1	18.4±5.7
24 h	18.2±4.6	16.5±4.3

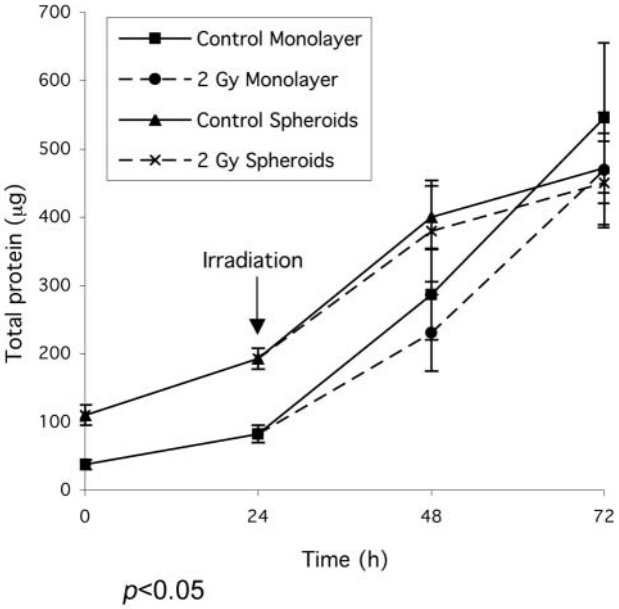

Figure 1. *Total amount of protein present as a function of time in the control MG-63 monolayer cells and those irradiated with a dose of 2 Gy and in the control spheroids and in those irradiated with this same dose. The data represent the means and standard deviations of 3 independent experiments in which 10 different trials were conducted in each experiment.*

1% agarose gel containing 0.5 µg/ml ethidium bromide at 25 V in TBE buffer (2 mM EDTA, pH 8.0; 89 mM Tris; 89 mM boric acid). The molecular weight marker used was a mixture of φX174 DNA - H*ae* III Digest (Finnzymes, Espoo, Finland) and λ DNA - H*ind* III Digest (Sigma Chemical Co.). Following electrophoresis, DNA was visualized by transilluminator and photographed by a Polaroid camera.

Statistical analyses. All statistical analyses not otherwise specified were carried out using the paired Student's *t*-test.

Results

Evaluation of cell damage

LDH release: Since LDH is released from the cytosol of damaged cells, the quantity of this release is an indicator of cell membrane damage. As can be seen in Table I, there were no differences in the enzyme leaked values expressed as a percentage of total LDH enzyme (*i.e.*, (extracellular)/{(extracellular)+(intracellular)}x100) in the control monolayer cells and spheroids or in the monolayer cells and spheroids exposed to 2 Gy of ionizing radiation, respectively, at all times tested. These results indicate that the exposure conditions used in the present study did not induce an increase in the release of LDH and thus did not damage MG-63 spheroids.

Growth assessment by total protein determination: As can be seen in Figure 1, there were no significant variations in total protein content and, consequently, in cell growth between control MG-63 monolayer cells and spheroids and their respective counterparts irradiated with 2 Gy of ionizing radiation.

One-dimensional ^{1}H-NMR measurements of whole MG-63 monolayer cells and spheroids and their respective perchloric acid extracts at 500 MHz. A representative 500 MHz ^{1}H-NMR experiment conducted on the control MG-63 monolayer cells and on those cells irradiated with 2 Gy of ionizing radiation is provided in Figure 2. One of the 5 500 MHz ^{1}H-NMR experiments conducted on the control MG-63 spheroids and on those spheroids after the same 2 Gy radiation dose is provided in Figure 3. All samples were taken 24 h after the irradiation itself. The spectra (in the range from 0 to 4.0 ppm) of the control and irradiated cells and of the control and irradiated spheroids, respectively, have the same general appearance. However, significant differences can, nonetheless, be noted. In order to better examine these differences, the spectra of each pair were normalized using the algorithm described above and the normalized spectrum of control MG-63 monolayer cells (Figure 2a) was subtracted from the normalized spectrum of those cells exposed to 2 Gy of ionizing radiation (Figure 2b). The normalized spectrum of the control spheroids (Figure 3a) was also subtracted from the normalized spectrum of those spheroids exposed to 2 Gy of radiation (Figure 3b). The difference spectrum of monolayer cells is shown in Figure 2c, while the difference spectrum of spheroids is shown in Figure 3c. In the difference spectra, intense peaks, indicating important variations between control and exposed cells and spheroids, can be observed. Of particular interest are the signals resonating at about 3.77 ppm (reduced glutathione; GSH), at about 3.60 ppm (inositol; Ino), between 3.41 and 3.25 ppm (taurine; Tau), at about 3.2 ppm (choline-containing metabolites including choline, phosphocholine and glycerophosphocholine; Cho), at about 3.03 ppm (creatine and phosphocreatine; Cr + PCr), between 2.34 and 2.04 ppm (β-γ-glutamine and glutamate; Glu), at about 1.48 ppm (alanine; Ala), at about 1.33 ppm (lactate; Lac) and between 0.90-1.30 ppm (CH_2 and CH_3 groups arising from methylene and methyl groups of fatty acyl chains of lipids, respectively; Lipids CH_2 and Lipids CH_3).

After the normalization procedure described above, these signals, which showed important qualitative variations, were simulated in order to obtain more quantitative information (29). The most significant variations in percent observed between the control and irradiated MG-63 monolayer cells and spheroids in the 5 separate experiments conducted are summarized in the histogram of Figure 4. The means and

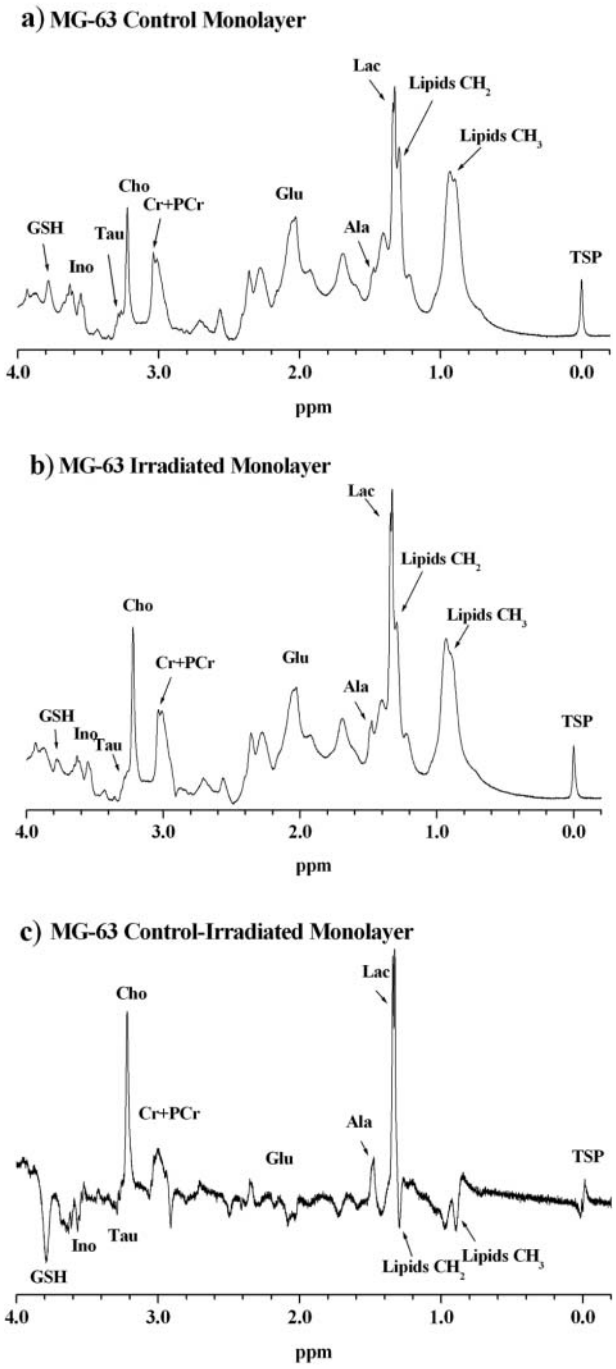

Figure 2. *Representative high resolution 500 MHz proton NMR spectra in the range from 0–4 ppm of MG-63 control monolayer cells (a) and of those cells exposed to 2 Gy of ionizing radiation (b) 24 h after irradiation. The resulting difference spectrum (irradiated - control/irradiated) of the monolayer cells exposed to 2 Gy is shown in (c). Only the metabolites in which important differences were observed are assigned. Abbreviations: GSH (reduced glutathione), Ino (inositol), Tau (taurine), Cho (choline-containing metabolites), Cr+PCr (creatine and phosphocreatine), Glu (glutamine and glutamate), Ala (alanine), Lac (lactate), CH_2 lipids (CH_2 chains of lipid fatty acids), CH_3 lipids (CH_3 chains of lipid fatty acids) and TSP (standard).*

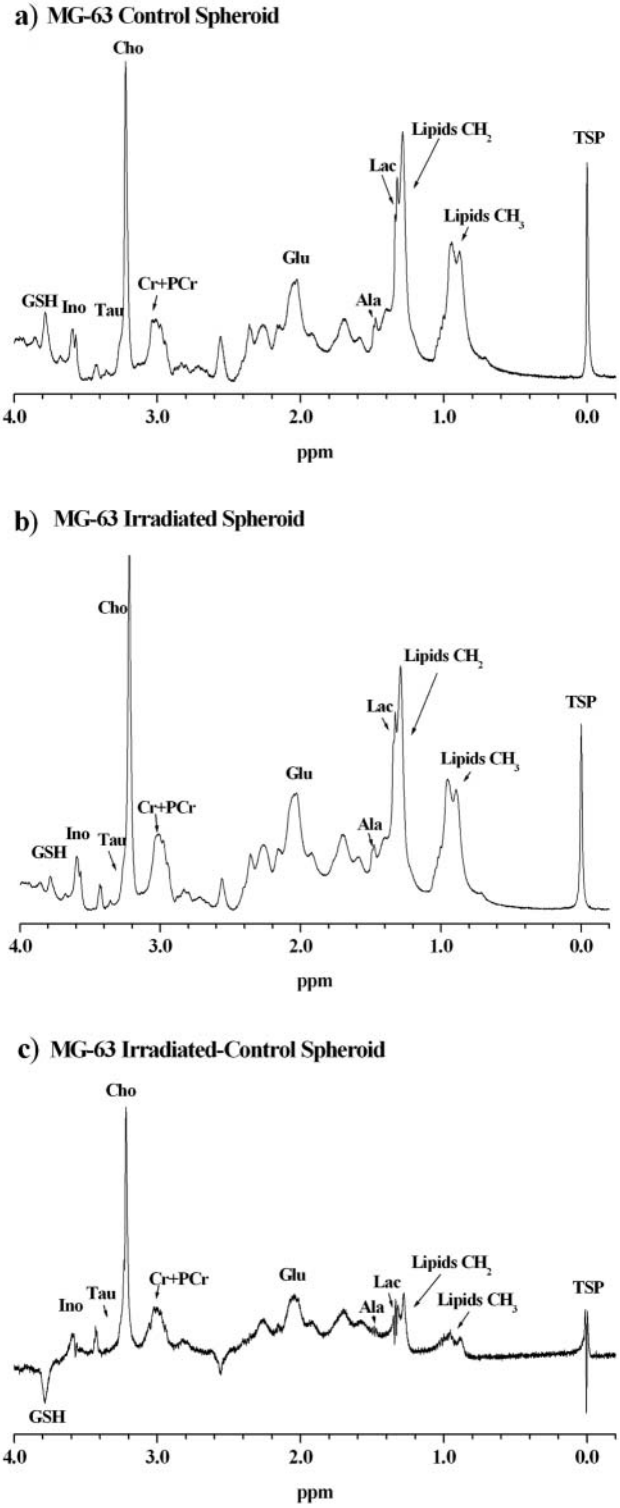

Figure 3. *Representative high resolution 500 MHz proton NMR spectra in the range from 0–4 ppm of MG-63 control spheroids (a) and of those spheroids exposed to 2 Gy of ionizing radiation (b) 24 h after irradiation. The resulting difference spectrum (irradiated - control/irradiated) of spheroids exposed to 2 Gy is shown in (c). The most evident metabolites are labelled and abbreviated as in Figure 2.*

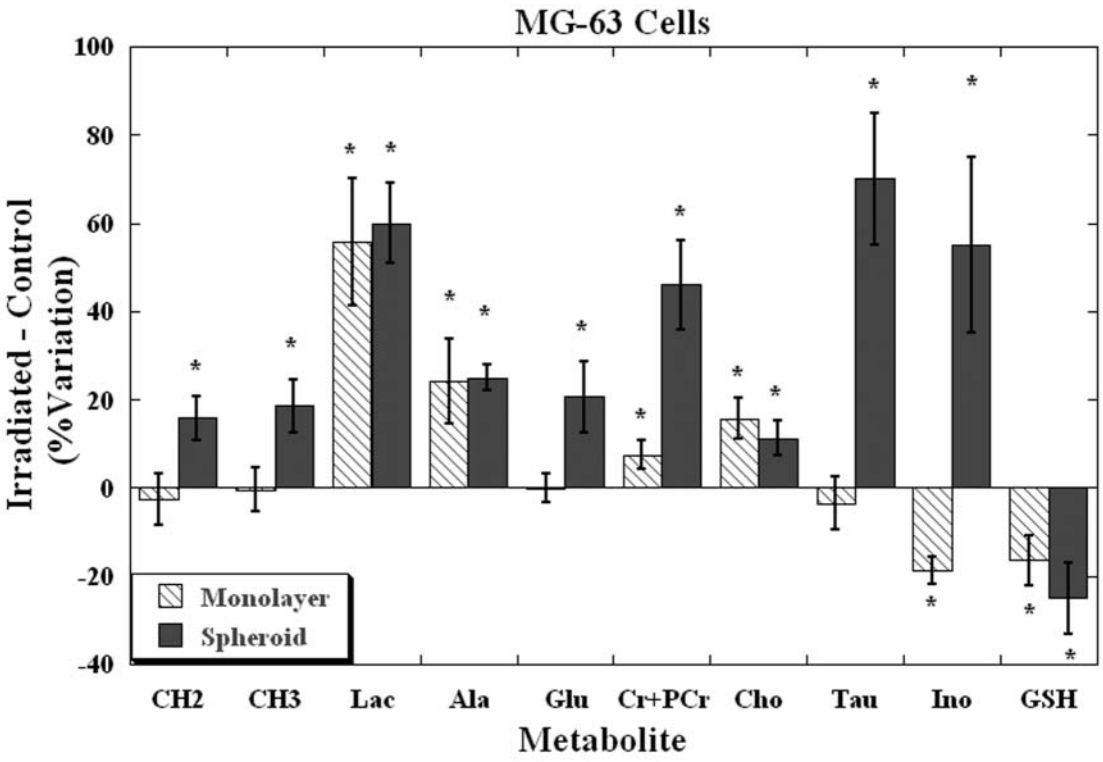

Figure 4. *Histogram summarizing the percent differences in the various metabolites of the MG-63 monolayer cells and spheroids exposed to a dose of 2 Gy. The means and standard deviatons of at least 5 separate experiments conducted at 500 MHz are shown. Only the metabolites in which important variations were found are graphed. The abbreviations are the same as those in Figure 2. The quantitative data presented were obtained after elaboration, as described in the text. All positive values indicate a greater amount of a metabolite in exposed cells with respect to controls ($p<0.05$). Asterisks indicate metabolites whose variations are statistically significant.*

standard deviations of these 5 experiments are presented. The differences were considered as significant ($p<0.05$). As can be seen in the figure, statistically significant increases in Lac, Ala, Cr+PCr and Cho and a significant decrease in GSH are present in both cells and spheroids. However, while significant increases in CH_2 and CH_3 mobile lipids, Glu, Tau and Ino were seen in the spheroids, no variations in CH_2 and CH_3 lipids, Glu or Tau were recorded in the MG-63 cells grown in monolayer after irradiation. In addition, a significant decrease rather than a significant increase in Ino was also noted in the monolayer cells with respect to the spheroids. For convenience, the variations in α-glutamine and glutamate and those in β-γ-glutamine and glutamate were summed together in the 5 experiments and presented in the histogram in the Glu column.

One of the 500 MHz ^{1}H-NMR experiments conducted on extracts of the control MG-63 monolayer cells and of those cells collected 24 h after a 2 Gy irradiation are shown in Figure 5 (a) and (b), respectively. Representative 500 MHz ^{1}H-NMR experiments conducted on extracts of the control MG-63 spheroids and on those spheroids collected after 24 h of a 2-Gy irradiation are depicted in Figures 6 (a) and (b), respectively. As can be seen, the spectra of the control and exposed monolayer cells and of the control and exposed spheroids, respectively, are quite similar. The means and standard deviations of the 5 extract experiments conducted in cells and spheroids are shown in the histogram presented in Figure 7. These extract results qualitatively confirm the trends observed in whole cells spheroids. Significant increases in the soluble metabolites Lac and Cho were seen in both the monolayer cells and the spheroids, while significant increases in Ala and Tau were observed only in spheroids, since monolayer cells presented no signficant variations in these metabolites. In addition, no significant variations were noted in Glu or GSH in either monolayer cells or spheroids. Finally, a significant decrease in Ino was observed in monolayer cells, while a significant increase in this metabolite was noted in spheroids. It should be noted that the results obtained in whole cells and extracts were quantitatively different. Although the reasons for these variations are not known, it may be hypothesized that, during extraction, some metabolites are lost while others are unmasked.

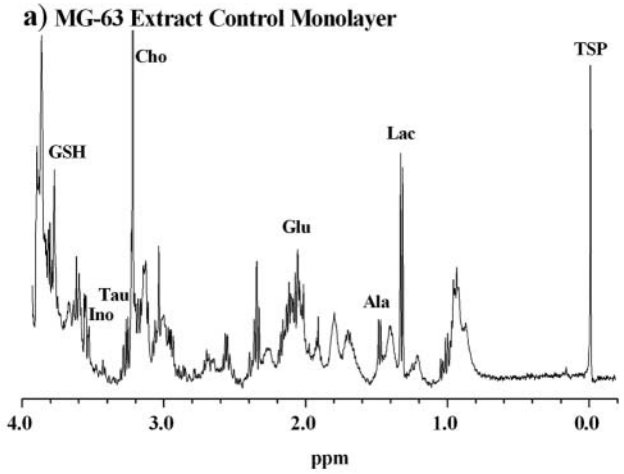

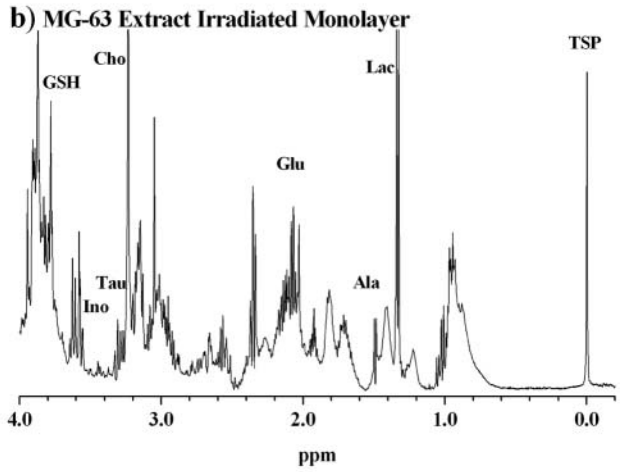

Figure 5. *Representative high resolution 500 MHz proton NMR spectra of perchloric acid extracts prepared from control MG-63 monlayer cells (a) and of those cells exposed to 2 Gy of ionizing radiation, 24 h after irradiation (b). The region between 0 and 4 ppm is shown. The most evident metabolites are labelled and abbreviated as in Figure 2.*

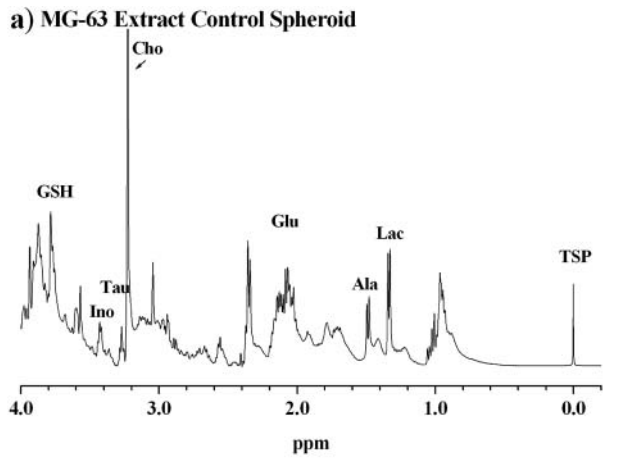

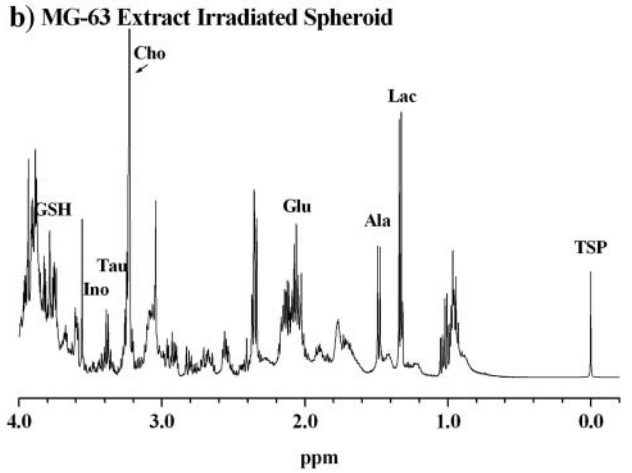

Figure 6. *Representative high resolution 500 MHz proton NMR spectra of perchloric acid extracts prepared from control MG-63 spheroids (a) and of those spheroids exposed to 2 Gy of ionizing radiation, 24 h after irradiation (b). The region between 0 and 4 ppm is shown. The most evident metabolites are labelled and abbreviated as in Figure 2.*

Two-dimensional ^{1}H-NMR measurements of whole MG-63 monolayer cells and spheroids at 500 MHz. In order to substantiate the data obtained with the 1-dimensional analyses, 2-dimensional measurements were conducted. Representative 2-dimensional ^{1}H-NMR spectra of MG-63 monolayer cells and spheroids exposed to 2 Gy of ionizing radiation, taken 24 h after the irradiation itself, are shown in Figure 8 (a) and (b), respectively. As can be seen, important cross-peaks related to fatty acyl chains are marked in the spectra, especially in light of the importance that variations in CH_2 and CH_3 lipids have on apoptosis. The signals examined in the TOCSY spectra of both monolayer cells and spheroids included those usually designated as A (0.9/1.3 ppm), B (1.3/2.1 ppm), C (2.0/5.4 ppm), D (2.8/5.4 ppm), E (1.3/1.6 ppm), F (1.6/2.3 ppm), L (0.9/2.1 ppm) and Z (0.9/1.5) (cholesterol). A, B, C, D and F showed no significant variations in monolayer cells with respect to controls (not shown), while important increases in these metabolites was observed in spheroids with respect to their controls (not shown). These data substantiate the important increase in CH_2 and CH_3 lipids observed in the exposed spheroids in the 1-dimensional experiments. In addition, it should be noted that, in the 2-dimensional spectra, it was possible to identify non-lipid peaks that also contributed to the CH_2 and CH_3 resonances in both monolayer cells and spheroids. In particular, the cross-peaks attributable to isoleucine (Ile, 1.0/2.1 ppm), leucine (Leu, 1.0/1.8 ppm), threonine (Thr, 1.3/4.3 ppm), valine (Val, 1.0/2.3 ppm) and fucose (FucI, 1.3/4.3 ppm, FucII, 1.2/4.3 ppm, FucIII, 1.4/4.3 ppm) were also identified. These amino acids and other macromolecules contributed to the CH_2 and CH_3 peak intensities, with fucose and threonine being the major contributors to these resonances.

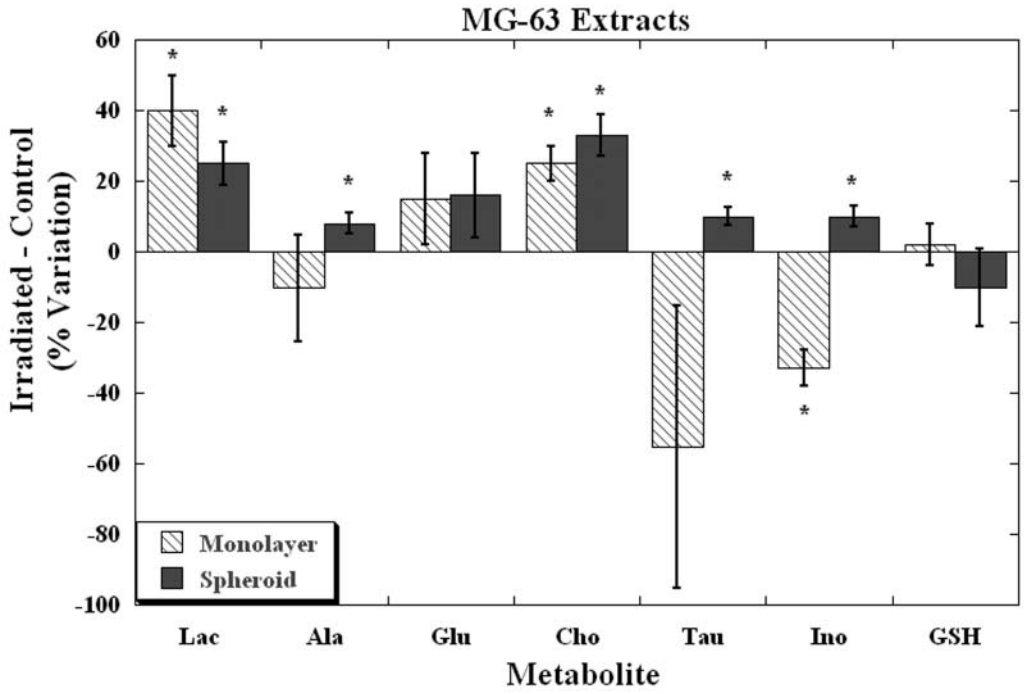

Figure 7. *Histogram summarizing the percent differences in the various metabolites of the perchloric acid extracts of MG-63 monolayer cells and spheroids exposed to a dose of 2 Gy. The means and standard deviations of 5 separate experiments conducted at 500 MHz are shown. Only the metabolites in which important variations were found are graphed. The abbreviations are the same as those in Figure 2. The quantitative data presented were obtained after elaboration, as described in the text. All positive values indicate a greater amount of a metabolite in exposed cells with respect to controls ($p<0.05$). Asterisks indicate metabolites whose variations are statistically significant.*

In order to determine the exact nature of the changes occurring in the choline-containing metabolites, the cross-peaks related to choline (Cho, 3.5/4.1 ppm), phosphocholine (PC, 3.6/4.2 ppm) and glycerophosphocholine (GPC, 2.2/3.8 ppm) were also examined in the TOCSY spectra of the control and exposed MG-63 monolayer cells and spheroids. As can be seen, the separation of the choline, phosphocholine and glycerophosphocholine signals was possible and increases in all 3 of these metabolites were present in both monolayer cells and spheroids when compared to their respective controls (not shown). These data confirm the 1-dimensional ^{1}H-NMR measurements of both whole cells and perchloric acid extracts of MG-63 monolayer cells and spheroids, which also showed similar increases in the choline-containing metabolites.

Two-dimensional ^{1}H-NMR measurements also resulted in the determination of increases in lactate (Lac, 1.3/4.1 ppm) and alanine (Ala, 1.5/3.8 ppm) in both exposed monolayer cells and spheroids with respect to their respective controls (not shown). In addition, important decreases in reduced glutathione (GSH, 2.9/4.6 ppm), as for the 1-dimensional spectra of the whole cells, were also observed in both exposed MG-63 monolayer cells and spheroids. The changes in inositol and taurine in the 1-dimensional spectra were also substantiated by the TOCSY spectra. Inositol (Ino, 3.3/3.6 ppm) decreased in monolayer cells and increased in the spheroids, while taurine (Tau, 3.3/3.5 ppm) did not show a significant variation in cells, but increased in the spheroids in both whole cells and extracts.

Determination of apoptosis

Hoechst 33258 staining: Apoptotic cells were evaluated in the MG-63 control and irradiated monolayer cells and spheroids by fluorescence microscopy utilizing the DNA stain Hoechst at 24 h after irradiation. In order to distinguish apoptotic cells, the nuclear morphological and ultrastructural parameters typical of this kind of cell death, previously described (30-32), were taken into account. Specifically, cells whose nuclei had a uniform and homogeneous distribution of uncondensed chromatin were considered as normal. Cells having clumped or condensed nuclear chromatin and/or chromatin marginalized against the nuclear membrane were considered as apoptotic. Representative fluorescence micrographs of control and irradiated MG-63 monolayer cells, as well as control and irradiated MG-63 spheroids, both stained with the nuclear dye Hoechst, are shown in Figure 9A (a) - (d), respectively.

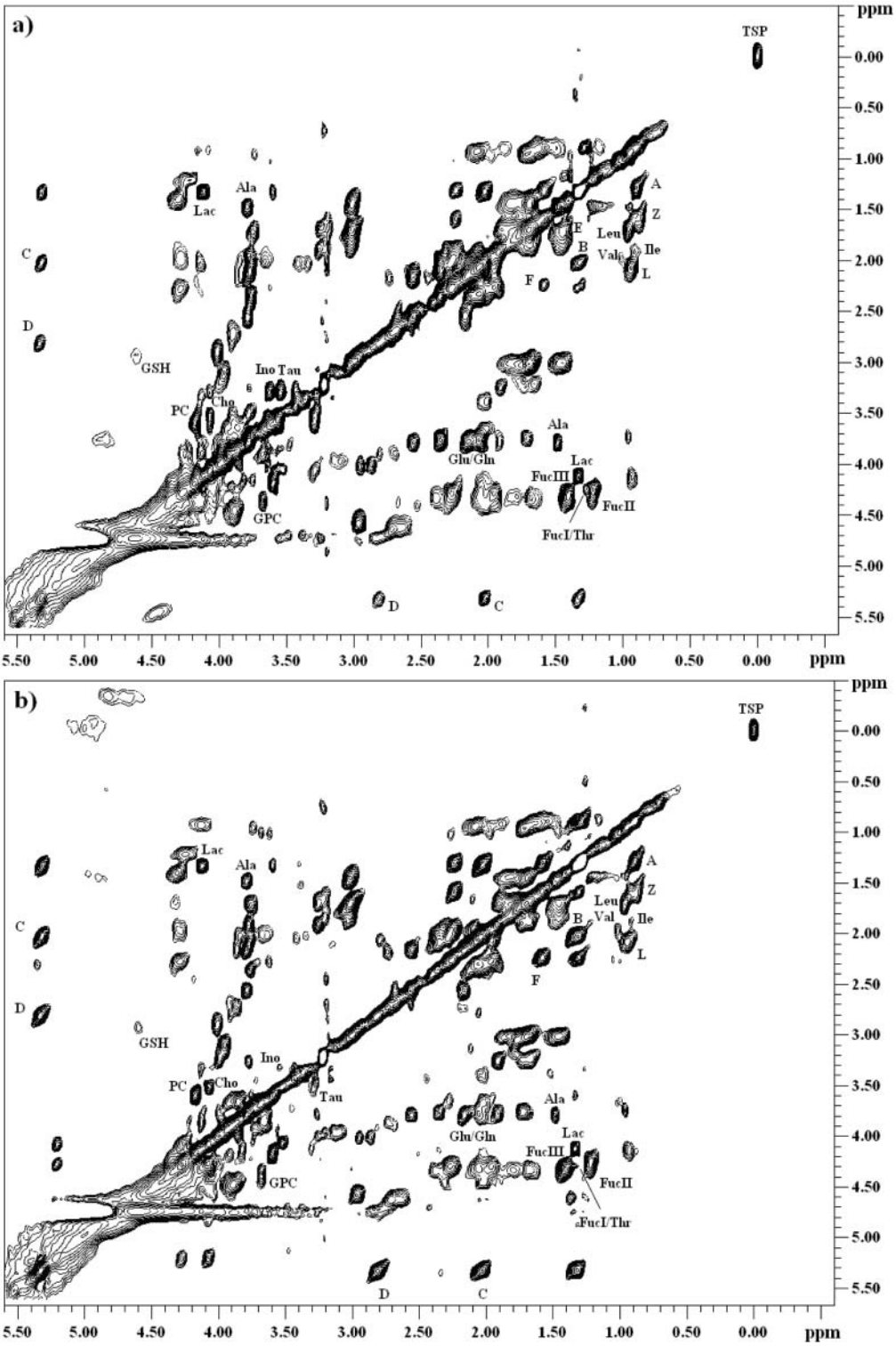

Figure 8. *^{1}H-NMR TOCSY spectra of MG-63 monolayer cells (a) and spheroids (b) exposed to 2 Gy of ionizing radiation, taken at 24 h after irradiation. Important cross-peaks related to lipids are marked as: A (0.9/1.3 ppm), B (1.3/2.1 ppm), C (2.0/5.4 ppm), D (2.8/5.4 ppm), E (1.3/1.6 ppm), F (1.6/2.3 ppm), L (0.9/2.1 ppm) and Z (0.9/1.5) (cholesterol). In addition, cross-peaks attributable to alanine (Ala, 1.5/3.8 ppm), isoleucine (Ile, 1.0/2.1 ppm), leucine (Leu, 1.0/1.8 ppm), valine (Val, 1.0/2.3 ppm), fucose (FucII, 1.2/4.3 ppm and FucIII, 1.4/4.3 ppm), fucose/threonine (FucI/Thr, FucI, 1.3/4.3 ppm and Thr, 1.3/4.3 ppm), inositol (Ino, 3.3/3.6 ppm), taurine (Tau, 3.3/3.5 ppm), choline (Cho, 3.5/4.1 ppm), phosphocholine (PC, 3.6/4.2 ppm), glycerophosphocholine (GPC, 2.2/3.8 ppm), lactate (Lac, 1.3/4.1 ppm) and reduced glutathione (GSH, 2.9/4.6 ppm) are also shown.*

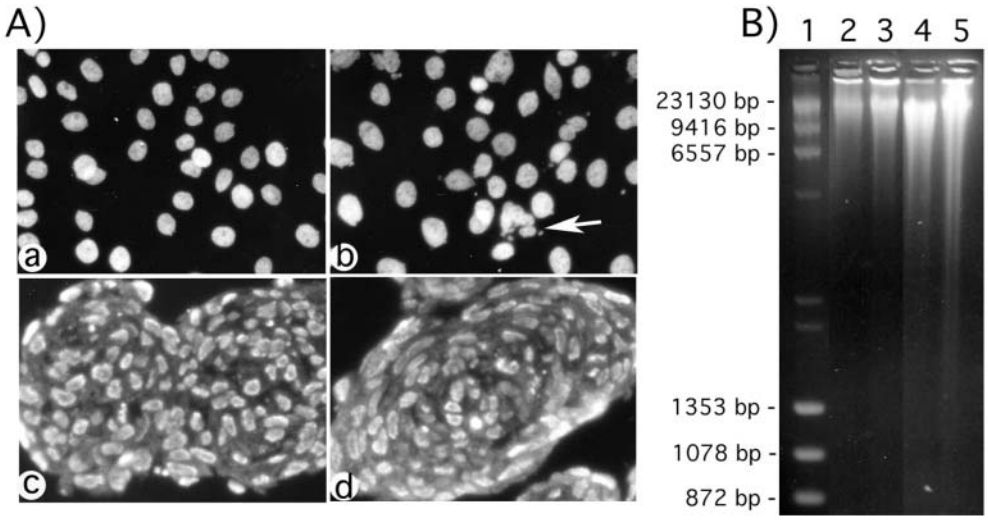

Figure 9. *A. Representative fluorescence micrographs of the MG-63 control monolayer cells (a), of those cells exposed to 2 Gy of ionizing radiation (b), of the MG-63 control spheroids (c) and of those spheroids exposed to 2 Gy of ionizing radiation (d) stained with the chromatin dye Hoechst. Samples were taken 24 h after irradiation. The arrow in (b) indicates multinucleated cells. The number of apoptotic cells was found to be very low in both the control and irradiated monolayer cells and spheroids ($p<0.05$). Magnification: (a) and (b) 670 X and (c) and (d) 1050 X. B. DNA gel electrophoresis of the control MG-63 monolayer cells (Lane 2), the control MG-63 multicellular spheroids (Lane 4), the monolayer cells irradiated with a dose of 2 Gy collected after 48 h of irradiation (Lane 3) and the irradiated spheroids also collected after 48 h (Lane 5). Lane 1 represents the size marker DNA (a mixture of φX174 DNA - Hae III Digest and λ DNA - Hind III Digest). No evidence of nucleosomal DNA fragments typical of apoptosis nor signs of necrosis are visible in all samples examined.*

The percentage of apoptotic as well as necrotic cells was very low (<2%) in both control and exposed monolayer cells and spheroids, indicating that cell death was not overtly induced by 2 Gy of ionizing radiation in either cell model investigated. However, as the figures also illustrate, the irradiated monolayer cells showed signs of damage while the exposed spheroids did not. The nuclei of the irradiated monolayer cells are swollen and are blebbled. In addition, multinucleation is also evident.

Analysis of DNA fragmentation by gel electrophoresis: The DNA gel electrophoresis of the control MG-63 monolayer cells (Lane 2), control MG-63 multicellular spheroids (Lane 4), monolayer cells irradiated with a dose of 2 Gy collected after 48 h of irradiation (Lane 3) and spheroids also irradiated with the same dose and collected after 48 h (Lane 5), are depicted in Figure 9B. Lane 1 represents the size marker DNA (a mixture of φX174 DNA - H*ae* III Digest and λ DNA - H*ind* III Digest). As can be seen, no evidence of nucleosomal DNA fragments could be detected in any sample studied, signifying that there was no apoptosis in either irradiated cells or spheroids. The typical DNA-gel ladder observed in apoptotic cells cannot be seen in any sample. In addition, no typical signs of necrosis were present in any sample. Experiments conducted after 7 days of irradiation gave similar results (data not shown).

Discussion

The results presented in this report seem to indicate that MG-63 monolayer cells and spheroids respond in a very different manner to 2 Gy of ionizing radiation. Specifically, the changes in CH_2 and CH_3 mobile lipids, taurine, inositol and glutamine/glutamate in the 2 cell models are quite diverse. As far as CH_2 and CH_3 mobile lipids are concerned, numerous researchers have demonstrated that the spectral peaks resonating at about 0.9 and 1.3 ppm, arising from methyl and methylene groups of fatty acyl chains of lipids, respectively, are related to cell death processes both *in vitro* and *in vivo* (33-39). In particular, these studies indicated that an accumulation of CH_2 and CH_3 mobile lipids occurred during apoptosis in different cell types, while necrosis did not result in such an accumulation. In addition, changes in CH_2 and CH_3 signal intensities have also been correlated to the progression of the apoptotic response (35). In this study, an increase in both CH_2 and CH_3 lipids was observed in irradiated MG-63 spheroids, while these 2 lipid moieties did not vary in the monolayer cells. Consequently, it may be speculated that radiation exposure triggers apoptosis in spheroids while it initiates another cell death process in monolayer cells. This hypothesis is quite reasonable since it is well-documented that ionizing

radiation can induce oxidative stress and that this type of stress can lead to both apoptosis and necrosis (40-43). The intensity of the stress can also shift cells from one mode of cell death to another (*e.g.*, apoptosis to necrosis) (44). Since spheroids are known to be more resistant than monolayer cells, it appears likely that the same dose of radiation can shift from apoptosis in spheroids to another type of cell death in monolayer cells. However, when cell death was investigated, it was determined that neither monolayer cells nor spheroids actually died. Thus, from these data, it may be speculated that the apoptotic triggering and initiation of a non-apoptotic cell death program were reversed in the MG-63 spheroids and monolayer cells, respectively. This hypothesis is substantiated by the important variations observed in antioxidant metabolites including taurine and GSH discussed in detail below. In addition, these results also underline the great sensitivity of ^{1}H-NMR in observing very subtle variations in cellular metabolites in response to ionizing radiation, observations which are not possible with other techniques.

It should also be pointed out that the 2-dimensional experiments conducted in this work showed that other macromolecules, such as polypeptides and amino acids (*e.g.*, leucine, isoleucine, alanine and threonine) and fucose contributed to the CH_2 and CH_3 resonances, especially in spheroids. Therefore, it cannot be excluded that the variations observed in these resonances in spheroids represent cell changes that are not exclusively related to apoptosis. For instance, it may be hypothesized that the changes in CH_2 and CH_3 resonances may be indicative of perturbations in the cytoskeleton or protein synthesis, phenomena in which polypeptides and amino acids play an important role. In such a case, the differences in behavior of the CH_2 and CH_3 resonances in the monolayer cells and spheroids may not be indicative of the triggering of a different type of cell death mechanism, but rather of different effects on the cytoskeleton or other important cellular proteins. This aspect is being investigated in our laboratory.

The taurine signal also responded differently to irradiation in the 2 cell models examined. In the spheroids, taurine increased significantly after 2 Gy of radiation while, in the monolayer cells, the quantity of this amino acid did not vary after irradiation. Taurine, which is found free in the cytosol, is especially abundant in cells involved in the inflammatory response and in cells exposed to elevated levels of oxidants. Derived from methionine and cysteine metabolism, taurine is known to play a pivotal role in numerous physiological functions, depending on the cell type, including osmoregulation, antioxidation, detoxification and stimulation of glycolysis and glycogenesis (45). It has been demonstrated that taurine exercises its function in cells through taurine chloramine, formed from the reaction between taurine and hypochlorous acid (46). Specifically, taurine chloramine prevents tissue damage induced by oxidants by inhibiting the further production of cytokines (46-48). Consequently, it may be hypothesized that the increase in taurine found in MG-63 spheroids irradiated with 2 Gy may be an attempt by these cells to counteract the oxidative stress and apoptotic triggering induced by ionizing radiation. Since overt apoptosis could not be documented in these spheroids, it may be postulated that the cellular response to this low dose of ionizing radiation was sufficient to block damage, revert apoptosis and ensure cell survival in these 3-dimensional systems. In monolayer cells, on the other hand, it may be hypothesized that the reversal of damage occurred through alternative repair mechanisms that do not involve taurine. Further investigation is required.

However, an alternative explanation for the increase in taurine observed in spheroids after 2 Gy of ionizing radiation should also be considered. As stated above, the amino acid taurine also plays an important role in osmoregulation. In fact, cells respond to the stress of hyperosmolarity by concentrating a large number of compatible organic osmolytes including sorbitol, betaine, inositol, glycerophosphocholine, and the free amino acids taurine, alanine, glycine, proline, glutamate, glutamine and aspartate (49, 50). However, many cell types preferentially accumulate taurine following osmotic perturbation (50). This accumulation allows for the maintenance of normal cell volume without the deleterious increase in intracellular inorganic ion concentration. Therefore, an alternative explanation for the increase in taurine observed in exposed MG-63 spheroids may be that irradiation induced cell damage and osmolytic dysregulation and that, in turn, this dysregulation was contrasted by taurine. In fact, it is well-known that ionizing radiation induces cell damaging reactive oxygen species (ROS) and that ROS can regulate taurine in various cell types (51, 52). In addition, it should also be recalled that taurine uptake occurs actively *via* the high-affinity, low-capacity, Na^+-, Cl^-- and pH-dependent transport system designated as TauT and taurine release is mediated by the volume-sensitive taurine efflux pathway (50). Perhaps radiation affects one or both of these transport mechanisms. Furthermore, it has been demonstrated that taurine release can be regulated by production of lysophosphatidylcholine (LPC) (53) and that the regulation of LPC production is mediated by protein kinase C (PKC) (54). Thus, ROS may also directly damage cell membrane lipids and cause osmolytic dysregulation, which is then counteracted by taurine. Again, in monolayer cells, it may be postulated that different osmoregulatory mechanisms, that do not involve taurine, are elicited as a consequence of exposure to ionizing radiation. This hypothesis seems reasonable, especially when considering the different spatial oraganization and cell-cell interaactions present in the 2 cell models. Nonetheless, further study is required.

Inositol also exhibited a different behavior in monolayer cells and spheriods after irradiation. In fact, in monolayer cells a significant decrease was observed, while in spheroids a significant increase was noted. Inositols are involved in cell signaling, especially in the phosphatidylinositol cycle (55). The initial event in this cycle is the binding of an agonist (such as a neurotransmitter, hormone, growth factor, *etc.*) to a receptor on the cell membrane surface. This binding leads to the breakdown of phosphatidylinositol diphosphate (PIP_2) to diacylglycerol (DAG) and inositol-1,4,5-triphosphate (IP_3). DAG activates protein kinase C (PKC) while IP_3 causes the release of Ca^{++} from non-mitochondrial stores, largely from the endoplasmic reticulum. Variations in the phosphatidylinositols can lead to perturbations in cell signaling and, as a result, in cell function. Thus, it appears that cells and spheroids have a different cell signaling response to 2 Gy of ionizing radiation. The exact meaning of these differences needs further investigation.

An alternative hypothesis for the differences observed in inositol, however, is again possible. As stated above, inositol is another important organic osmolyte (50). Therefore, it may be postulated that the decrease in inositol in cells and the increase in this metabolite in spheroids is due to differences in the osmoregulatory response of the 2 cell systems to 2 Gy of ionizing radiation. Although the exact mechanisms of osmoregulation in cells and spheroids are not clearly understood, it is, nonetheless, apparent that bi- and tri-dimensional growth requires very diverse cell volumes, intracellular and extracellular ionic concentrations, ion channel structure and function, *etc.* Consequently, it is evident that the response to radiation stress is also very different in the 2 cell models investigated. Further study is necessary.

Glutamine/glutamate also behaved differently in cells and spheroids exposed to 2 Gy of ionizing radiation. Although it is not possible to separate the glutamine and glutamate resonances in the present work and, consequently, impossible to determine which of the 2 was actually changing, it is, nonetheless, important that variations in these metabolites took place. Once again, diverse hypotheses may be suggested for these variations. First, glutamine and glutamate are substrates for GSH production and thus take part in the synthesis of this important antioxidant molecule. Therefore, it is possible that cells and spheroids have different antioxidant defense mechanisms and that, as a result, glutamine and glutamate take part in the reaction of these systems to ionizing radiation in a different manner. These amino acids may also be involved in the protection of cells from apoptosis (56, 57). In fact, this protection occurs through the maintenance of an adequately high ATP concentration (58). Consequently, these amino acids help prevent programmed cell death by supplying some of the additional energy necessary for survival in cells subjected to apoptotic stimuli. Therefore, although the precise mechanisms are unclear, the different response of glutamine and glutamate observed with ^{1}H-NMR again points to a diverse repair of the ionizing radiation-induced oxidative damage and cell death triggering in MG-63 cells and spheroids. Finally, glutamine/glutamate may also take part in osmoregulation, since these amino acids are important osmolytes as well (50).

In conclusion, this study indicates that monolayer cells and spheroids of the MG-63 osteosarcoma cell line respond in a different manner to the same dose (2 Gy) of ionizing radiation. In particular, these 2 cell models appeared to have a different cell death response. The ^{1}H-NMR spectra of spheroids showed the signs of apoptotic triggering (accumulation of CH_2 and CH_3 mobile lipids), while the spectra of monolayer cells showed no such programmed cell death response. In addition, the different behavior of taurine, glutamine/glutamate and inositol in monolayer cells and spheroids suggests the existence of either a very different antioxidant response to ionizing radiation of the 2 cell models and/or very diverse osmoregulatory mechanisms of cells and spheroids. Since both hypotheses are very reasonable, further study is necessary. Nonetheless, it is apparent that ^{1}H-NMR can be a very sensitive and useful tool in examining, non-invasively, the different response of monolayer cells and 3-dimensional spheroids to ionizing radiation.

Acknowledgements

The authors wish to thank Mr. Giacomo Monteleone for irradiation of the monolayer cells and spheroids. This work was partially financed by a grant from the Istituto Superiore di Sanità, Italy, to MTS (Project N. 9B/F/3 entitled "Evaluation of cellular response to radiation in 3-dimensional model systems – spheroids").

References

1 Santini MT and Rainaldi G: Three-dimensional spheroid model in tumor biology. Pathobiol *67*: 148-157, 1999.

2 Santini MT, Rainaldi G and Indovina PL: Apoptosis, cell adhesion and the extracellular matrix in the three-dimensional growth of multicellular tumor spheroids. Crit Rev Oncol Hematol *36*: 75-87, 2000.

3 Barba I, Cabañas ME and Arùs C: The relationship between nuclear magnetic resonance-visible lipids, lipid droplets, and cell proliferation in cultured C6 cells. Cancer Res *59*: 1861-1868, 1999.

4 Cooper WA, Bartier WA, Rideout DC and Delikatny EJ: ^{1}H NMR visible lipids are induced by phosphonium salts and 5-fluorouracil in human breast cancer cells. Magn Reson Med *45*: 1001-1010, 2001.

5 Santini MT, Romano R, Rainaldi G, Filippini P, Bravo E, Porcu L, Motta A, Calcabrini A, Meschini S, Indovina PL and Arancia G: The relationship between ^{1}H-NMR mobile lipid intensity and cholesterol in two human tumor multidrug resistant cell lines (MCF-7 and LoVo). Biochim Biophys Acta *1531*: 111-131, 2001.

6 Bollard ME, Xu J, Purcell W, Griffin JL, Quirk C, Holmes E and Nicholson JK: Metabolic profiling of the effects of D-galactosamine in liver spheroids using ^{1}H NMR and MAS-NMR spectroscopy. Chem Res Toxicol *15*: 1351-1359, 2002.

7 Thews O, Zywietz F, Lecher B and Vaupel P: Quantitative changes of metabolic and bioenergetic parameters in experimental tumors during fractionated irradiation. Int J Radiat Oncol Biol Phys *45*: 1281-1288, 1999.

8 Iliakis G, Wang Y, Guan J and Wang H: DNA damage checkpoint control in cells exposed to ionizing radiation. Oncogene *22*: 5834-5847, 2003.

9 Suzuki K, Ojima M, Kodama S and Watanabe M: Radiation-induced DNA damage and delayed induced genomic instability. Oncogene *22*: 6988-6993, 2003.

10 Benderitter M, Vincent-Genod L, Pouget JP and Voisin P: The cell membrane as a biosensor of oxidative stress induced by radiation exposure: a multiparameter investigation. Radiat Res *159*: 471-483, 2003.

11 Watters D: Molecular mechanisms of ionizing radiation-induced apoptosis. Immunol Cell Biol *77*: 263-271, 1999.

12 Santini MT, Rainaldi G and Indovina PL: Multicellular tumour spheroids in radiation biology. Int J Radiat Biol *75*: 787-799, 1999.

13 Dubessy C, Merlin JL, Marchal C and Guillemin F: Spheroids in radiobiology and photodynamic therapy. Crit Rev Oncol Hematol *36*: 179-192, 2000.

14 Filippovich IV, Sorokina NI, Robillard N and Chatal JF: Radiation-induced apoptosis in human ovarian carcinoma cells growing as a monolayer and as multicell spheroids. Int J Cancer *72*: 851-859, 1997.

15 Sutherland RM and Durand RE: Cell contact as a possible contribution to radiation resistance of some tumours. Br J Radiol *45*: 788-789, 1972.

16 Olive PL and Durand RE: Drug and radiation resistance in spheroids: cell contact and kinetics. Cancer Meta Rev *13*: 121-138, 1994.

17 Meredith JE, Fazeli B and Schwartz MA: The extracellular matrix as a cell survival factor. Mol Biol Cell *4*: 953-961, 1993.

18 Romano R, Santini MT and Indovina PL: A time-domain algorithm for NMR spectral normalization. J Magn Reson *146*: 89-99, 2000.

19 Callies R, Sri-Pathmanathan RM, Ferguson DYP and Brindle KM: The appearance of neutral lipid signals in the ^{1}H-NMR spectra of a myeloma cell line correlates with the induced formation of cytoplasmic lipid droplets. Magn Reson Med Biol *29*: 546-550, 1993.

20 Rosi A, Luciani AM, Matarrese P, Arancia G, Viti V and Guidoni L: ^{1}H-MRS lipid signal modulation and morphological and ultrastructural changes related to tumor cell proliferation. Magn Reson Med *42*: 248-257, 1999.

21 Hwang TL and Shaka AJ: Water suppression that works. Excitation sculpting using arbitrary wave-forms and pulsed-field gradients. J Magn Reson *112*: 275-279, 1995.

22 Mountford CE, Lean CL and MacKinnon WB: The use of proton MR in cancer pathology. Annu Rep NMR Spectrosc *27*: 173-215, 1993.

23 Behar KL and Ogino T: Assignment of resonances in the ^{1}H spectrum of rat brain by two-dimensional shift correlated and J-resolved NMR spectroscopy. Magn Reson Med *17*: 285-303, 1991.

24 Berners-Price SJ, Sant ME, Christopherson RI and Kuchel PW: ^{1}H and ^{31}P NMR and HPLC studies of mouse L1210 leukemia cell extracts: the effect of Au(I) and Cu(I) diphosphine complexes on the cell metabolism. Magn Reson Med *18*: 142-158, 1991.

25 Braunschweiler L and Ernst RR: Coherence transfer by isotropic mixing: application of proton correlation spectroscopy. J Magn Reson *53*: 521-528, 1983.

26 Griesinger C, Otting G, Wüthrich K and Ernst RR: Clean TOCSY for ^{1}H spin system identification in macromolecules. J Am Chem Soc *110*: 7870-7872, 1988.

27 Drobny G, Pines A, Sinton S, Weitkamp D and Wemmer D: Fourier transform multiple quantum NMR. Faraday Div Chem Soc Symp *13*: 49-55, 1979.

28 Bax A and Davis DG: MLEV-17-based two-dimensional homonuclear magnetization transfer spectroscopy. J Magn Reson *65*: 355-366, 1985.

29 van den Boogart A, Ala-Korpela M, Jokisaari J and Griffiths JR: Time and frequency domain analysis of NMR data compared: an application to 1D ^{1}H spectra of lipoproteins. Magn Reson Med *31*: 347-358, 1994.

30 Bär PR: Apoptosis – The cell's silent exit. Life Sci *59*: 369-378, 1996.

31 Oberhammer FA, Froschl G, Tiefenbacher R, Inayat-Hussain SH, Cain K and Stopper H: A topical issue of microscopy research and technique. Microsc Res Tech *34*: 247-258, 1996.

32 Inayat-Hussain SH, Cohen GM and Cain K: A reappraisal of the role of Zi^{++} in TGF-β1-induced apoptosis in primary hepatocytes. Cell Biol Toxicol *15*: 381-387, 1999.

33 Hakumäki JM and Brindle KA: Techniques: visualizing apoptosis using nuclear magnetic resonance. Trends Pharmacol Sci *24*: 146-149, 2003.

34 Blankenberg FG, Storrs RW, Naumovski L, Goralski T and Spielman D: Detection of apoptotic cell death by proton nuclear magnetic resonance spectroscopy. Blood *87*: 1951-1956, 1996.

35 Blankenberg FG, Katsikis PD, Storrs RW, Beaulieu C, Spielman D, Chen JY, Naumovski L and Tait JF: Quantitative analysis of apoptotic cell death using proton nuclear magnetic resonance spectroscopy. Blood *89*: 3778-3786, 1997.

36 Al-Saffar NMS, Titley JC, Robertson D, Clarke PA, Jackson LE, Leach MO and Ronen SM: Apoptosis is associated with triacylglycerol accumulation in Jurkat T-cells. Br J Cancer *86*: 963-970, 2002.

37 Lehtimäki KK, Valonen PK, Griffin JL, Väisänen TH, Gröhn OHJ, Kettunen MI, Vepsäläinen J, Ylä-Herttuala S, Nicholson J and Kauppinen RA: Metabolic changes in BT4C rat gliomas undergoing ganciclovir-thymidine kinase gene therapy-induced programmed cell death as studied by ^{1}H-NMR spectroscopy *in vivo*, *ex vivo* and *in vitro*. J Biol Chem *278*: 45915-45923, 2003.

38 Hakumäki JM, Poptani H, Sandmair A-M, Ylä-Herttuala S and Kauppinen RA: ^{1}H MRS detects polyunsaturated fatty acid accumulation during gene therapy of glioma: implications for the *in vivo* detection of apoptosis. Nat Med *5*: 1323-1327, 1999.

39 Griffin JL, Lehtimäki KK, Valonen PK, Gröhn OHJ, Kettunen MI, Ylä-Herttuala S, Pitkänen A, Nicholson JK and Kauppinen RA: Assignment of ^{1}H nuclear magnetic resonance visible polyunsaturated fatty acids in BT4C gliomas undergoing ganciclovir-thymidine kinase gene therapy-induced programmed cell death. Cancer Res *63*: 3195-3201, 2003.

40 Agrawal A, Choudhary D, Upreti M, Rath PC and Kale RK: Radiation induced oxidative stress: I. Studies in Ehrlich solid tumor in mice. Mol Cell Biochem *223*: 71-80, 2001.
41 Lyng FM, Seymour CB and Mothersill C: Oxidative stress in cells exposed to low levels of ionizing radiation. Biochem Soc Trans *29*: 350-353, 2001.
42 Galan A, Garcia-Bermejo L, Troyano A, Vilaboa NE, Fernandez C, de Blas E and Aller P: The role of intracellular oxidation in death induction (apoptosis and necrosis) in human promonocytic cells treated with stress inducers (cadmium, heat, X-rays). Eur J Cell Biol *80*: 312-320, 2001.
43 Mishra KP: Cell membrane oxidative damage induced by gamma-radiation and apoptotic sensitivity. J Environ Pathol Toxicol Oncol *23*: 61-66, 2004.
44 Abend M: Reasons to reconsider the significance of apoptosis for cancer therapy. Int J Radiat Biol *79*: 927-941, 2003.
45 Stapleton PP, O'Flaherty L, Redmond HP and Bouchier-Hayes DJ: Host defense – a role for the amino acid taurine? J Parenter Enter Nutri *22*: 42-48, 1998.
46 Marcinkiewicz J, Grabowska A, Bereta J and Stelmaszynska T: Taurine chloramine, a product of activated neutrophils, inhibits *in vitro* generation of nitric oxide and other macrophage inflammatory mediators. J Leukoc Biol *58*: 667-674, 1995.
47 Barua M, Liu Y and Quinn MR: Taurine chloramine inhibits inducible nitric oxide synthase and TNF-alpha gene expression in activated alveolar macrophages: decreased NF-kappaB activation and IkappaB kinase activity. J Immunol *167*: 2275-2281, 2001.
48 Liu Y and Quinn MR: Chemokine production by rat alveolar macrophages is inhibited by taurine chloramine. Immunol Lett *80*: 27-32, 2002.
49 Burg MB: Molecular basis for osmoregulation of organic osmolytes in renal medullary cells. J Exp Zool *268*: 171-175, 1994.
50 Lambert IH: Regulation of the cellular content of the organic osmolyte taurine in mammalian cells. Neurochem Res *29*: 27-63, 2004.
51 Lambert IH: Reactive oxygen species regulate swelling-induced taurine efflux in NIH3T3 mouse fibroblasts. J Membr Biol *192*: 19-32, 2003.
52 Ørtenblad N, Young JF, Oksbjerg N, Nielsen JH and Lambert IH: Reactive oxygen species are important mediators of taurine release from skeletal muscle cells. Am J Physiol Cell Physiol *284*: C1362-C1373, 2003.
53 Lambert IH and Falktoft B: Lysophosphatidylcholine induces taurine release from HeLa cells. J Membr Biol *176*: 175-185, 2000.
54 Lambert IH and Falktoft B: Lysophosphatidylcholine-induced taurine release in HeLa cells involves protein kinase activity. Comp Biochem Physiol Part A *130*: 577-584, 2001.
55 Vance DE: Phospholipid metabolism and cell signalling in eucaryotes. *In*: Biochemistry of Lipids, Lipoproteins and Membranes. Vance DE, Vance J (eds). Amsterdam, Elsevier Science Publishers, pp. 205-240, 1991.
56 Papaconstantinou HT, Hwang KO, Rajaraman S, Hellmich MR, Townsend CM and Ko TC: Glutamine deprivation induces apoptosis in intestinal epithelial cells. Surgery *124*: 152-160, 1998.
57 Papaconstantinou HT, Chung DH, Zhang W, Ansari NH, Hellmich MR, Townsend CM and Ko TC: Prevention of mucosal atrophy: role of glutamine and caspases in apoptosis in intestinal epithelial cells. J Gastrointest Surgery *4*: 416-423, 2000.
58 Windmueller HG: Glutamine utilization by the small intestine. Adv Enzymol *53*: 201-237, 1982.

Received September 28, 2005
Accepted November 16, 2005